REPORT ON EXPERIMENT SI-1773

ROUND 4/2008 – 03-08/10/2008 – 15 SHIFTS

LOCAL CONTACT:	FRANCESCO D'ACAPITO
MAIN PROPOSER:	FRANCESCO DI BENEDETTO
TEAM MEMBERS (PRESENT AT ESRF):	MAURIZIO ROMANELLI, MASSIMO INNOCENTI, LUCA PARDI, GIORDANO MONTEGROSSI, GARBIELE FORNACIAI

Experimental details

The SI1773 experiment follows and integrates the SI1593 experiment, carried out at BM08 in Winter 2007. In that occasion, the most relevant standards, the reference Fe-bearing quartz samples and many industrial raw and processed samples were investigated both in the near-edge (XANES) and in the extended (EXAFS) regions, opportunely switching between the Transmission and Fluorescence mode.

During the present experiment, systematic ReflEXAFS measurements have been carried out at room temperature on selected quartz surfaces, doped through chemical etching with Fe(II) and Fe(III).

The following Table 1 summarises the whole experimental data set obtained (in blue the measurements acquired in SI1593)

Table 1 – analysed samples

name	exp	type	name	exp	type
Standard compounds			**Single crystal model compounds**		
Cellulose	Si1593	powders	amet	Si1593	single crystal
Co-ferrite	Si1593	powders	ame_re	Si1593	single crystal
hematite	Si1593	powders	quarzo_r	Si1593	single crystal
Fe	Si1593	powders	ame2	Si1773	single crystal
Iron Chloride	Si1593	powders	amet	Si1773	single crystal
ferrhydrite	Si1593	powders	quarzo2	Si1773	single crystal
goethite	Si1593	powders	quarzoz	Si1773	single crystal
Na-silicate	Si1593	powders	quarzo_z2	Si1773	single crystal
Fe oxalate	Si1593	powders	quarzo_z2b	Si1773	single crystal
Li-silicate	Si1593	powders	quarzo_z3b	Si1773	single crystal
Fe sulphate	Si1593	powders			
stannite	Si1593	powders	**Model compounds**		
wustite	Si1593	powders	qzc	Si1593	powders
almandine	Si1773	powders	qzc2	Si1593	powders
Fe oxalate	Si1773	powders	qzch	Si1593	powders
hematite	Si1773	powders	qzcm	Si1593	powders
			qzr	Si1593	powders
industrial			qzrfe	Si1593	powders
cem	Si1593	powders	qzrm	Si1593	powders
serena	Si1593	powders			
cotto	Si1593	powders			
cottom	Si1593	powders			
inerti	Si1593	powders			
inertim	Si1593	powders			
orafo	Si1593	powders			
orm	Si1593	powders			

The four groups are classified according to the following definitions: 1) Standard compounds (for valence, coordination, bond in XAS); 2) model compounds (powders having certified provenance, features and composition); 3) Single crystal model compounds (large Fe-bearing quartz crystal, cut along a specific surface); 4) industrial compounds (coming from real processes, not necessarily monophasic).

The investigated surfaces were the following: a) quarzo ⇨ 100; b) amethyst ⇨ 101; c) quarzo_z ⇨ 001.

These were analysed as prepared (polished without etching) and after chemical treatment, according to the following list:

1) quarzo_r ⇨ + Fe(III)
2) ame_re ⇨ + Fe(III)
3) ame2 ⇨ + Fe(II)
4) quarzo2 ⇨ + Fe(II)
5) quarzoz ⇨ + Fe(III) --- changes under the beam ---
6) quarzo_z2 ⇨ + Fe(II)
7) quarzo_z2b ⇨ + Fe(II)
8) quarzo_z3b ⇨ + Fe(III)

In the following sections, a preliminary survey of the data is presented.

ReflEXAFS data (XANES)

The XANES spectra of quartz and amethyst reveal an evident shift of about + 2 eV of the former with respect to the latter (**Fig. 1**);

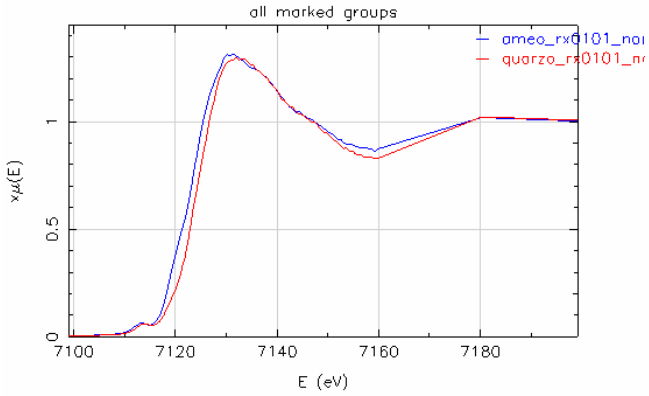

Figure 1 - XANES spectra of quartz and amethyst

After the analysis of the small pre-edge peak, performed assuming the summation of 2 pseudo voigt peaks, we are able to qualitatively see a double peak evident in the case of amethyst and hematite and only a single peak for quartz (Fig. 2). A quantitative refinement yield the values reported in Table 2.

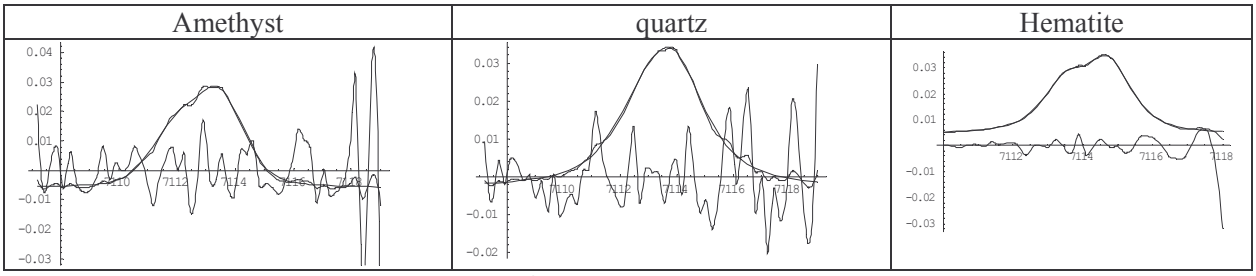

Figure 2 – Analysis of the pre-edge peak

Table 2 – Quantitative analysis of the pre-edge peak

Sample	Line 1		Line 2	
	Amplitude	Pos (eV)	Amplitude	Pos (eV)
Quartz	0.009(1)	7112.2(2)	0.028(1)	7113.8(2)
Amethyst	0.018(1)	7111.9(2)	0.029(1)	7113.5(2)
Hematite	0.018(1)	7113.5(2)	0.026(1)	7114.8(2)

In the case of quartz, we see that the pre-edge peak contains two components at 7112 and 7113 eV. The same happens for amethyst but with a component at 7112 considerably higher. The data on the amethyst resemble those of hematite but with a shift of -1.5 eV. The reference data associated to the spectra (reference in hema_x and ferif_x01) exhibit a shift of about 0.2 eV.

ReflEXAFS data (EXAFS)

Quartz has a better quality than amethyst. In the raw EXAFS spectrum it is evident the presence of high frequency oscillations (marks in the k space spectra) that correspond to those in hematite. The model sill be thus a mix between oxidized Fe (presumably corresponding to the phase linked to the surface) and hematite. The results are shown in Figure 3 and Table 3.

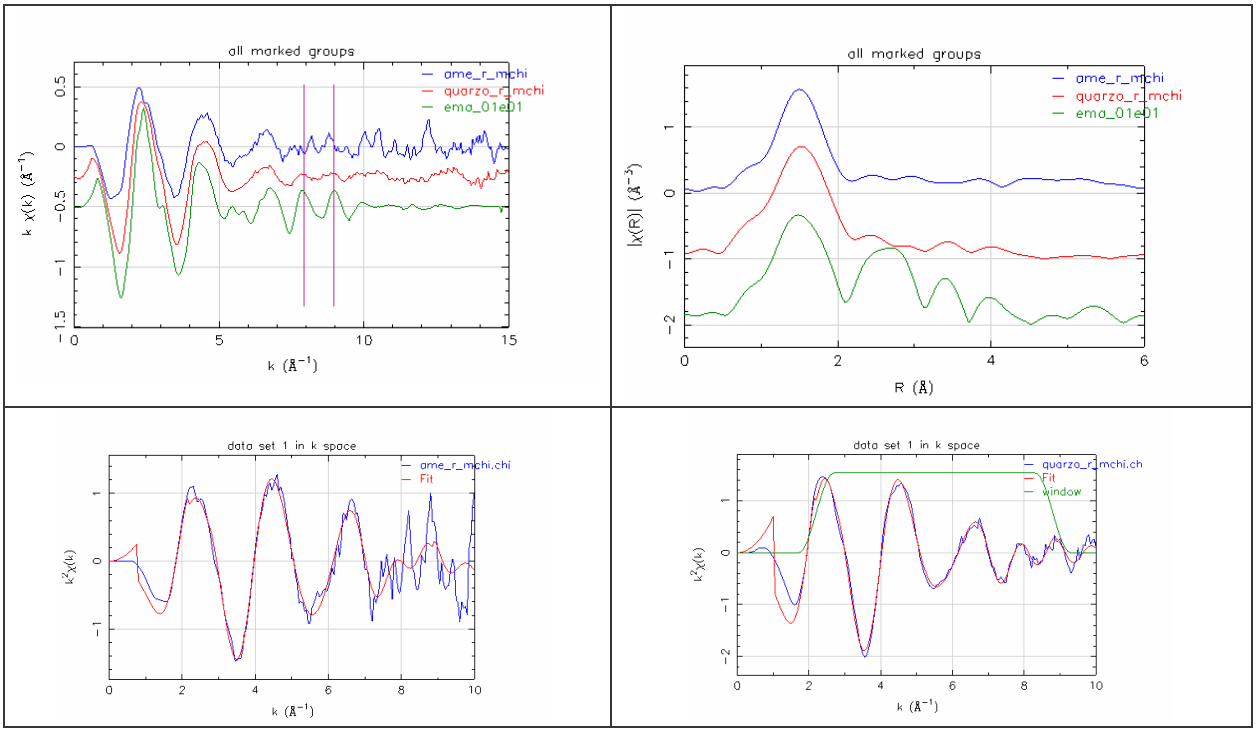

Figure 3 – EXAFS data on amethyst, quartz and hematite samples

Sample	Fe-O I	Fe-O II	expansion	% hematite
Hematite	1.93(2)	2.10(2)	0.000	100
Quartz	1.91(2)	2.07(2)	0.007(6)	25(6)
Amethyst	1.90(2)	2.07(2)	0.01(1)	20 (10)

Table 3 – quantitative EXAFS data on amethyst, quartz and hematite samples

We can see that in both cases the contribution of the hematite form is of about 20%. The remainder of Fe is in an oxidized form presumably linked to the surface and exhibiting a bond length shorter than that observed

for hematite. It is worth to make a statistical analysis to state if effectively there are 2 Fe-O distances or just 1. The two models appear equivalent from a statistical point of view (Tab. 4).

Table 4 – statistical analysis of the considered models

2 shells		1 shell	
NI	1.9	N	5.0
RI	1.88	R	1.99
NII	2.5		
RII	2.06		
Σ2	0.0008	Σ2	0.0128
ν	1	ν	3
χ^2	1	χ^2	2.2

EXAFS data (powders)

Model compounds: qzc and qzcm
These compounds (related by the fact that qzcm is qzc after mechanical treatment in laboratory) are clearly distinct in their features: qzc appears similar to hematite, whereas qzcm has marked similarities with metallic Fe (Fig. 4). Bond Fe-O distances are 1.92(3) and 2.05(3) Å, thus confirming the ferric state.

Model compounds: qzr and qzrm
EXAFS spectra reveal a strong similarity of qzr and qzrm samples (again related by the fact that qzrm is qzr after mechanical treatment in laboratory). Respirable dusts, therefore, seem not modified after grinding. However, both spectra suggest the present of a stable component of metallic Fe (~45(5)%). The most abundant interaction can be again described as amorphous Fe oxide, with a Fe-O bond distance of 1.96(3) Å, thus again Fe^{3+} (Fig. 5).

Industrial compounds: orafo and orafo_m
A mixed Fe-O and metallic Fe contribution is already present in the raw sample (representative of the sands used for casting gold alloys). After the mechanical treatment in laboratory the amount of metallic Fe increases (Fig. 6), from 25(2) to 57(5) %. The Fe-O shell occurs at 2.00(3) Å, thus confirming the ferric nature of the Fe-O amorphous contribution.

Industrial compounds: inerti and inerti_m
The EXAFS spectra of these samples (representative of the building materials), before and after mechanical treatment in laboratory, reveal an homogeneous Fe oxide phase. No evident grinding effects are observed. A pre-edge analysis (Tab. 5) was thus operated: positions and shapes of the peaks excellently agree with those of hematite, thus confirming the trivalent state for Fe. EXAFS is adequately fit by 30(5)% ematite and 70(5) % Fe-O phase.

Industrial compounds: cotto and cotto_m
In the case of samples representative of terra cotta industry, again raw and treated samples are quite similar. However the similarity to the hematite standard is no longer valid: Fe, therefore is conceivably in a different mineral phase. The pre-edge analysis (Tab. 6) confirm that a shift toward lower energy values has occurred (-1 eV) and thus Fe is in the divalent state. The EXAFS fit evidences Fe coordinated in the first shell with 4 O at a distance of 2.09(3).

<table>
<tr><td> 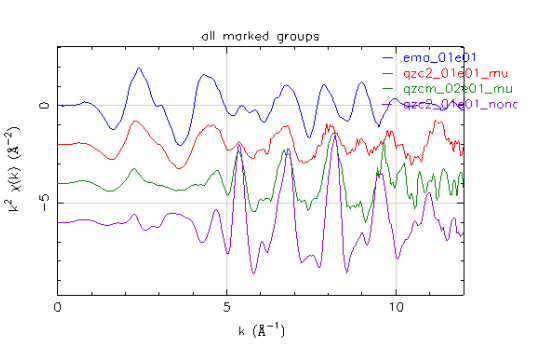
</td><td>qzc:
55% Fe-O
29% Hematite
16% Fe metallico
(uncertainty 10%).

Qzcm:
55% Fe met
45% Fe-O
(uncertainty 5%)

(Fe-O means amorphous oxide)</td></tr>
<tr><td> 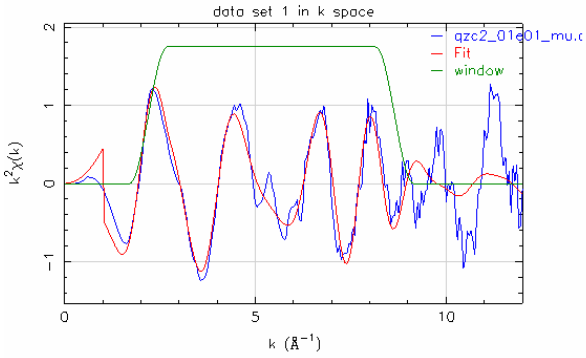
</td><td> 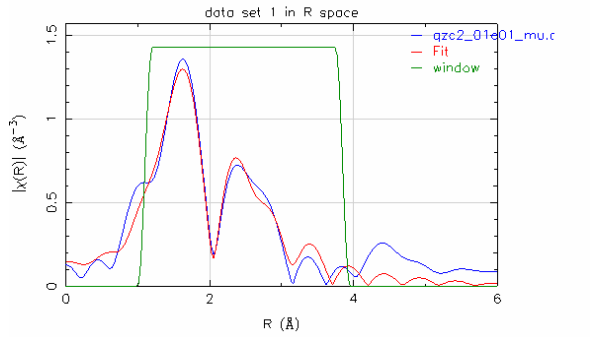
</td></tr>
<tr><td>QZC exafs</td><td>QZC Fou</td></tr>
<tr><td> 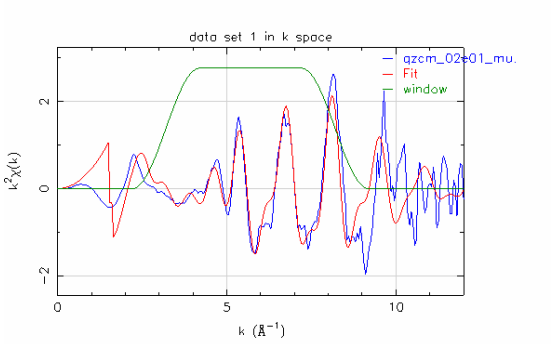
</td><td> 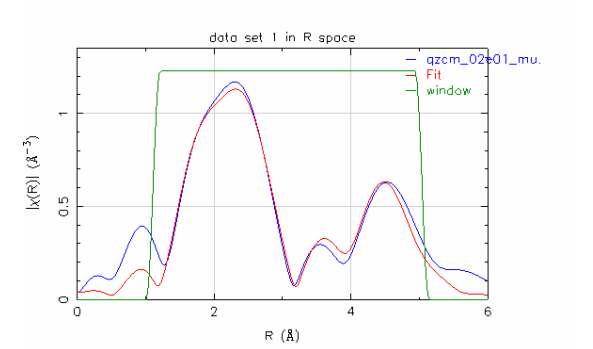
</td></tr>
<tr><td>QZCm exafs</td><td>QZCm Fou</td></tr>
</table>

Figure 4 – EXAFS data on qzc and qzcm

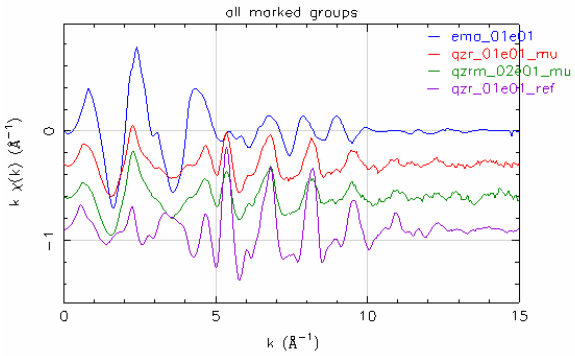

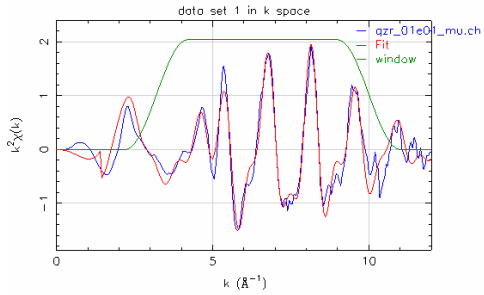

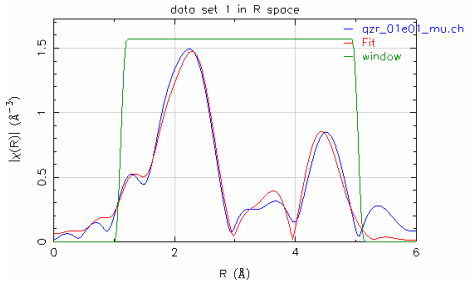

Qzr exafs	Qzr fourier

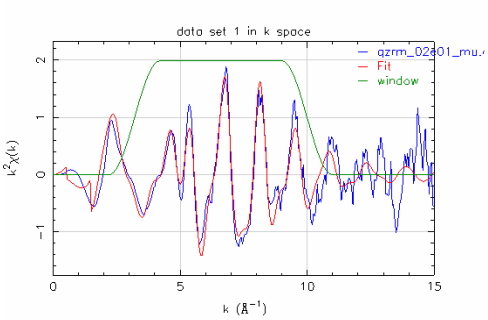

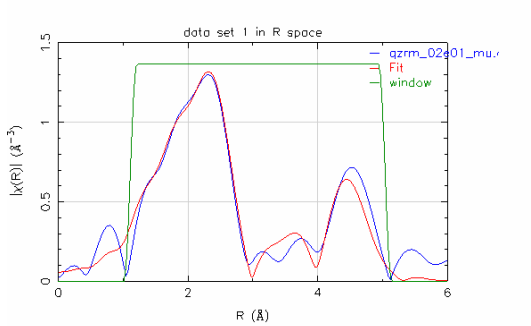

Qzrm exafs	Qzrm fourier

Figure 5 – EXAFS data on qzr and qzrm

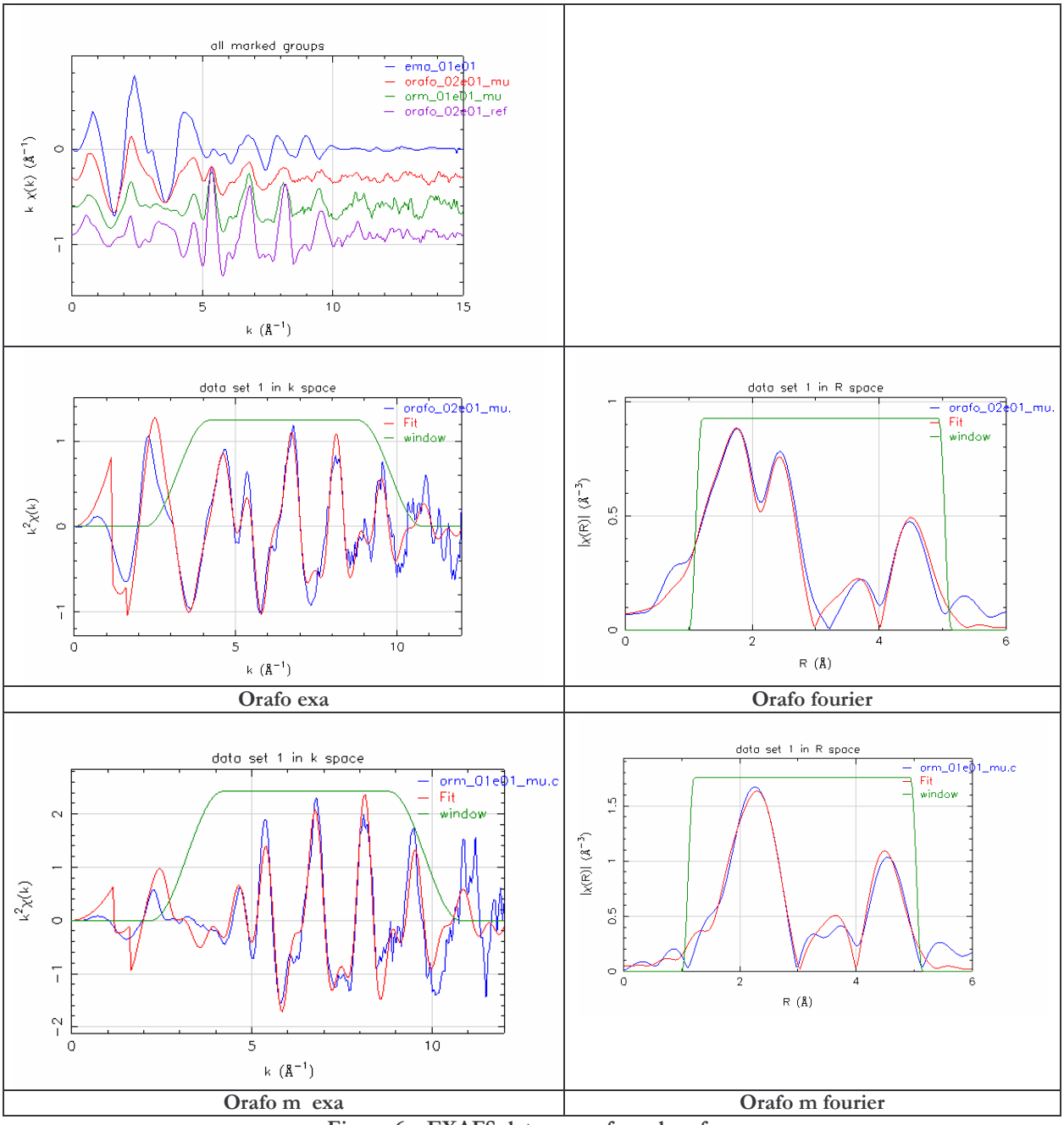

Figure 6 – EXAFS data on orafo and orafom

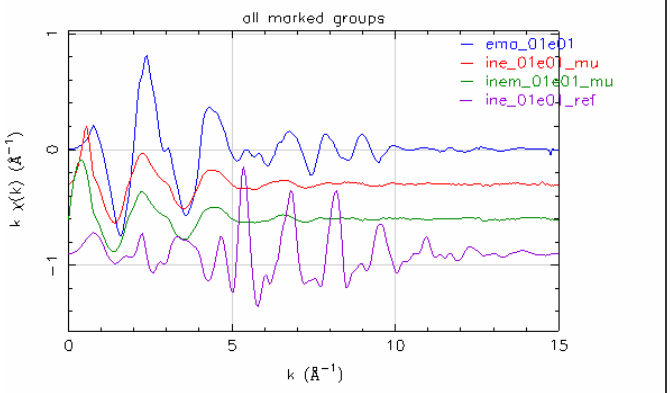

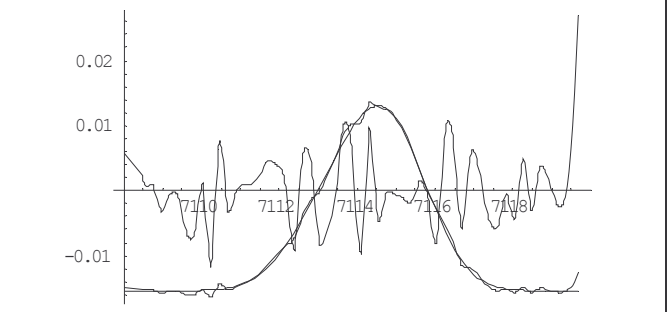

Inerti

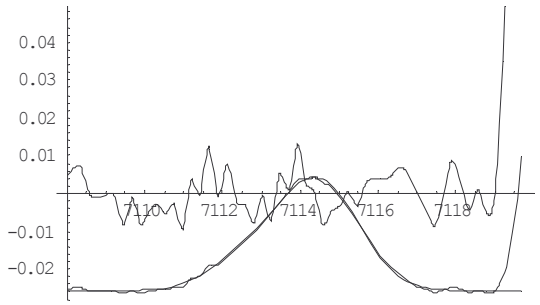

Inerti m

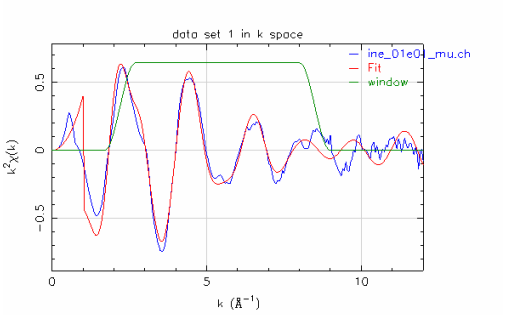

inerti exa

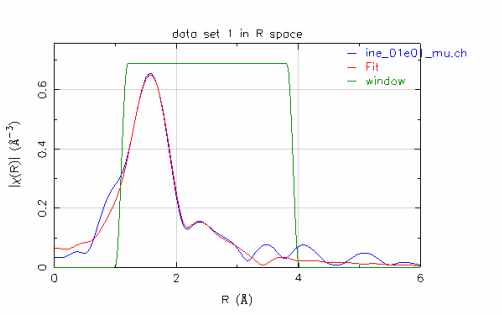

inerti fourier

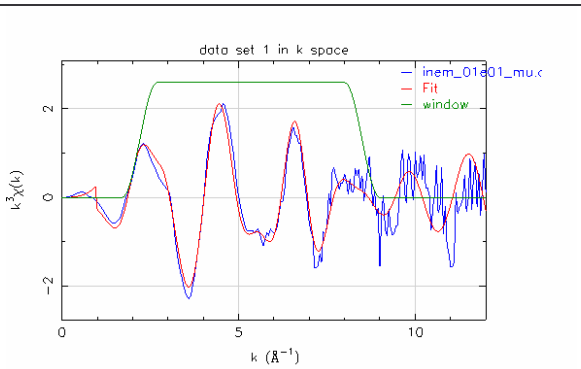

Inerti_m exa

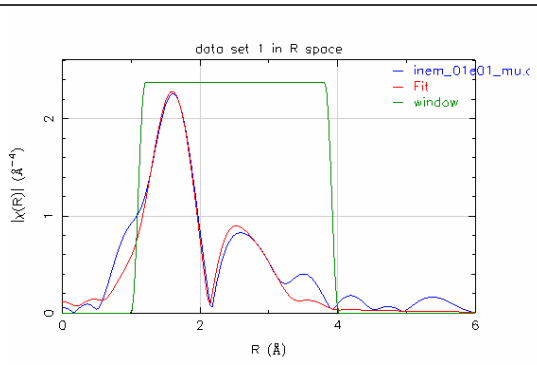

Inerti_m fourier

Figure 7 – EXAFS data on inerti and inerti_m

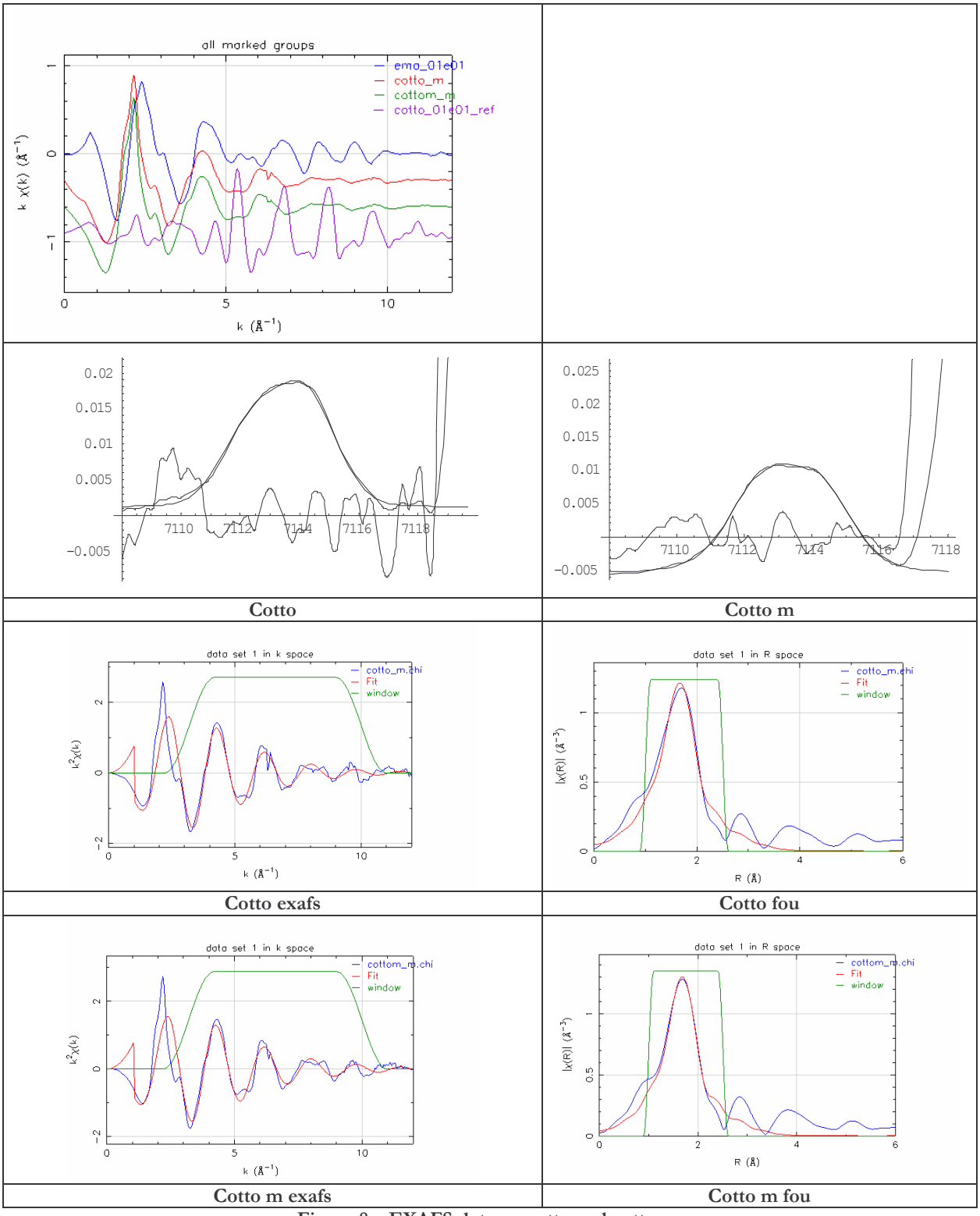

Figure 8 – EXAFS data on cotto and cotto_m

Table 5 – quantitative EXAFS data on inerti and inerti_m

Sample	Line 1		Line 2	
	Amplitude	Pos (eV)	Amplitude	Pos (eV)
Inerti	0.011(1)	7113.3(2)	0.024(1)	7114.8(2)
Inerti m	0.0096(1)	7112.8(2)	0.027(1)	7114.5(2)
Hematite	0.018(1)	7113.5(2)	0.026(1)	7114.8(2)

Table 6 – quantitative EXAFS data on cotto and cotto_m

Sample	Line 1		Line 2	
	Amplitude	Pos (eV)	Amplitude	Pos (eV)
Cotto	0.011(1)	7112.4(2)	0.015(1)	7114.3(2)
Cotto m	0.013(1)	7112.5(2)	0.013(1)	7114.2(2)
Hematite	0.018(1)	7113.5(2)	0.026(1)	7114.8(2)

Fe valence in amethyst

A Fe-K edge EXAFS study on Fe valence in amethyst was undertaken with the aim of describing the chemical and structural characteristics of Fe impurities at the local scale. This investigation was performed on a large single crystal of Brazilian amethyst cut parallel to the (1, 1, 0) natural surface, successively polished down to 1 μm.

Spectra were collected at room temperature, and energy calibration was checked by measuring a Fe metallic foil before and after each spectrum. EXAFS data were compared with *ab-initio* calculations based on the Density Functional Theory, carried out by using the VASP code. The full potential projected augmented-wave (PAW) method with Local Spin Density Generalized Gradient Approximation (LSD-GGA) was used as implemented in VASP.

X-ray Absorption Near-Edge Structure (XANES)

The X-ray Absorption Near Edge Structure (XANES) spectra of the sample (Figure 9) reveal that the edge of the amethyst sample is at a slightly lower energy that of hematite (Fe^{3+}) and well above that of wustite (Fe^{2+}). This suggests that Fe is predominantly in the 3+ valence state.

The peaks appearing in the pre-edge region (7108-7118 eV, inset of Fig. 2) have been best fitted with a double pseudo-voigt line. We found evidence of two lines at 7114.6(2) eV with an amplitude (relative to normalized edge jump) of 11(1)%, and at 7112.9(3) with an amplitude of 2(1)%. Accordingly, we can derive that Fe is present predominantly in the 3+ state with a possible contribution from Fe^{2+} estimated to be less than 20%.

Extended X-ray Absorption Fine Structure (EXAFS)

The EXAFS data (Fig. 10) provide quantitative results on the local geometry around Fe. The best fit result indicates that Fe is coordinated to 3.1(5) O atoms at 1.78(2) Å and with a Debye-Waller factor of 0.015(4) $Å^2$. This latter value is considerably higher respect to what observed for Fe-bearing silicate glasses suggesting the presence of a multiplicity of Fe-O distances. Moreover, Fe-O bond length is considerably shorter than what observed in literature for Fe in silicate glasses.

DFT calculations were performed to compare and interpret the EXAFS experimental findings. In particular, we have simulated the environment of a Fe^{4+} and a Fe^{3+} ion substituting for Si in its site in the structure of quartz. In the latter case the extra positive charge was compensated with a neutralizing background charge on the cell. Calculations where calibrated with known standard structures.

We found values by DFT for the Fe-O distances in both Fe^{3+} and Fe^{4+} replacement models, at 1.84 and 1.78 Å, respectively. These data are in good agreement with the experimental findings on the average Fe-O bond lengths in tetrahedral coordination (1.89 Å and 1.80 Å for Fe^{3+} and Fe^{4+}, respectively) in Na_5FeO_4 and Na_4FeO_4 crystals.

The comparison of the DFT computational and EXAFS experimental data allows, therefore, to evidence that the first shell Fe-O distance in amethyst could be in principle compatible with the four-valent state, although the present XANES and most of the literature agree to point out that Fe occurs mainly in the trivalent state. On the other hand, the multiplicity of sites ascertained by the high Debye-Waller value can be easily explained in terms of a variegate speciation of Fe: Fe^{4+} and Fe^{3+}, variably compensated, replace Si inducing a multiplicity of local structural distortions.

The experimental distance, conceivably smaller than that expected for trivalent Fe in four-fold coordination, could be related to the presence of charge compensating cations (Li^+, H^+) that have been proposed in literature to realize charge neutral complexes with Fe^{3+}.

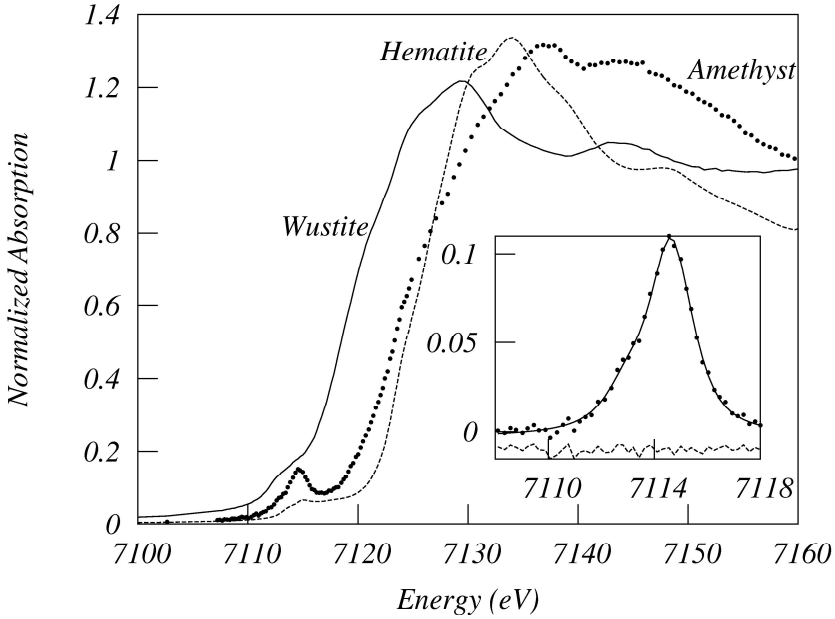

Figure 9 - XANES spectra of amethyst sample compared with model compounds for Fe^{2+} (wustite) and Fe^{3+} (hematite). In the inset the pre-edge peak of amethyst sample is reported (dots) together with the fit with 2 lines (line) and the residual (dashed line).

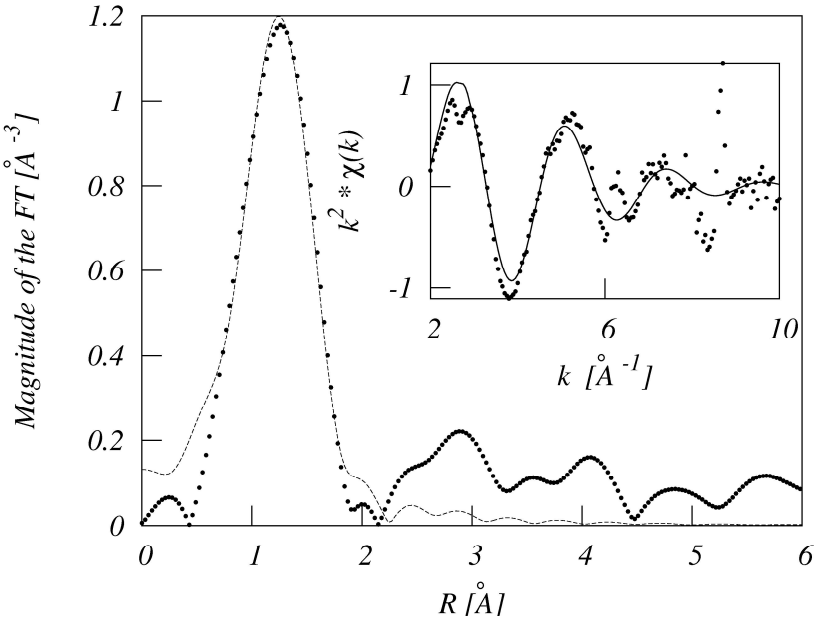

Figure 10 - Fourier Transform of the EXAFS data (shown in the insert). The transform was carried out in the interval k=[1.1-8.0]Å^{-1} with a k^2 weight.

Preliminary conclusions

During the SI1593 and SI1773 experiments, we were successful in obtaining relevant data for the speciation of Fe in natural and industrial samples of crystalline silica:

1) the first coordination shell of Fe in amethyst, which was found to be located in the structural tetrahedral site of Si, with a Fe-O distance of 1.78(2) Å, was fully defined. These data were also confirmed by DFT calculations (Di Benedetto et al., submitted). No evidences of occupancy of other sites were detected;

2) the relationships between the quartz surfaces and Fe(II) and Fe(III) ions, deposited through a chemical etching, were determined; indeed, the tendency of these ions to clusterise to form Fe-oxide phases was ascertained, even if the deposited amount is lowered down to concentrations able to cover just a fraction of a monolayer;

3) the presence of Fe ions in all industrial and standard quartz samples was revealed. Samples were found to exhibit different speciation features, as a phenomenological function of granulometry and industrial/laboratory mechanical ageing. The consequent Fe bioavailability in breathable dusts would results largely variable in terms of its amount and reactivity.

FIRENZE, APRIL 2009